

Green Chemistry

Accepted Manuscript



This is an *Accepted Manuscript*, which has been through the Royal Society of Chemistry peer review process and has been accepted for publication.

Accepted Manuscripts are published online shortly after acceptance, before technical editing, formatting and proof reading. Using this free service, authors can make their results available to the community, in citable form, before we publish the edited article. We will replace this *Accepted Manuscript* with the edited and formatted *Advance Article* as soon as it is available.

You can find more information about *Accepted Manuscripts* in the [Information for Authors](#).

Please note that technical editing may introduce minor changes to the text and/or graphics, which may alter content. The journal's standard [Terms & Conditions](#) and the [Ethical guidelines](#) still apply. In no event shall the Royal Society of Chemistry be held responsible for any errors or omissions in this *Accepted Manuscript* or any consequences arising from the use of any information it contains.

ARTICLE

Continuous Production of Sugars from Pyrolysis of Acid-Infused Lignocellulosic Biomass

Cite this: DOI: 10.1039/x0xx00000x

Dustin L. Dalluge,^{ab} Tannon Daugaard,^{ab} Patrick Johnston,^{ab} Najeeb Kuzhiyil,^{ab} Mark Wright,^{ab} and Robert C. Brown^{ab}Received 00th January 2012,
Accepted 00th January 2012

DOI: 10.1039/x0xx00000x

www.rsc.org/

Although pyrolysis of carbohydrate-rich biomass should theoretically yield large amounts of sugar, the presence of alkali and alkaline earth metals (AAEMs) in most biomass prevents this from happening. Even in small amounts, AAEM strongly catalyzes the fragmentation of holocellulose to light oxygenates compared to the thermally-induced breaking of glycosidic bonds that yield anhydrosugars. The concept of AAEM passivation, by which the catalytic activity of AAEMs can be suppressed to enhance thermal depolymerization of lignocellulose to sugars, has been previously established at the microgram scale using batch reactors. The feasibility of increasing sugar yield via AAEM passivation has not been previously demonstrated at the kilogram scale in a continuous flow reactor. The goal of this research is to demonstrate the enhanced production of sugars from AAEM passivated feedstocks in a continuous auger pyrolyzer at the kilogram scale. Alkali and alkaline earth metal passivation prior to pyrolysis increased total sugars from red oak by 105% compared to conventional pyrolysis, increasing from 7.8 wt. % to 15.9 wt. % of feedstock. Light oxygenates and non-condensable gases (NCGs) simultaneously decreased 45%, from 27.1 wt. % to 14.7 wt. % of feedstock as a result of AAEM passivation. Similarly, AAEM passivation of switchgrass increased total sugars by 259%, from 4.5 wt. % to 16.2 wt. % of feedstock, while the light oxygenates and NCGs decreased by 48%, from 20.0 wt. % to 10.5 wt. % of feedstock. An undesirable outcome of AAEM passivation was an increase in char production, increasing by 65% and 30% for pyrolysis of red oak and switchgrass, respectively. Loss of lignin-derived phenolic compounds from the bio-oil can explain 67% and 38% of the increase in char for red oak and switchgrass, respectively. The remaining 33% char increase for red oak (3.1 wt. % char) and 62% char increase for switchgrass (4.0 wt. % char) appear to be from carbonization of sugars released during pyrolysis of acid-infused biomass.

1. Introduction

Sugars can be readily converted into biofuels, but sugars derived from starch and sugar crops have limited availability for fuels production. In principle, more plentiful supplies of sugars can be obtained from cellulosic biomass.^{1, 2} Although enzymatic and acid hydrolysis have received most of the attention for the production of sugars from cellulose, purely thermal processes are also possible. In particular, fast pyrolysis can depolymerize cellulose to anhydrosugars such as levoglucosan (LG).^{3, 4} Practical exploitation of thermal depolymerization of plant polysaccharides has been stymied by the presence of alkali and alkaline earth metals (AAEMs) inherent to most lignocellulosic biomass. Alkali and alkaline earth metals dramatically decrease the yield of anhydrosugars by catalysing pyranose and furanose ring fragmentation leading to increased yields of less desirable light oxygenates and non-condensable gases (NCGs).^{3, 5, 6}

Experiments at the microgram scale have demonstrated that pretreatment of biomass with carefully controlled quantities of sulphuric or phosphoric acid prior to pyrolysis allows almost 60% of the cellulose in lignocellulosic biomass to convert to anhydrosugars.⁷ The pretreatment process, known as AAEM passivation, consists of adding just enough sulphuric or phosphoric acid to convert all of the AAEM cations into thermally stable sulphates or phosphates. Conversion to thermally stable salts significantly reduces the catalytic activity of the AAEM cations, which would otherwise fragment biomass carbohydrates to light oxygenates and NCGs. Alkali and alkaline earth metal passivation appears to produce acid salts of AAEM cations,⁷ such as potassium hydrogen sulphate (KHSO₄), which have a buffering effect. The combination of AAEM passivation and buffering allows the preferential cleavage of glycosidic bonds rather than fragmentation of pyranose rings.^{6, 8} The amount of acid required for passivation is stoichiometric with respect to the AAEM content of the

biomass.⁷ Thus, the quantity of acid required is very small, especially for low ash content feedstocks such as red oak. For example, the red oak used in this work required only 0.4 wt. % sulphuric acid on a dry biomass basis to achieve maximum production of anhydrosugars.

Alkali and alkaline earth metal passivation requires relatively little water and subsequent drying compared to attempts to remove AAEM via washing.⁹⁻¹⁴ Water can present a major input both in terms of operating costs and energy, therefore water use should be minimized to make the process more economically feasible. The biomass-to-water ratios used in the reviewed literature for washing or infusion of acid catalysts ranged from 1:3 to 1:25 in batch systems, whereas the ratio used in the present work was as low as 1:1 for red oak. For AAEM passivation, water is used only to the extent necessary to homogeneously distribute the acid throughout the biomass. It is therefore likely that the biomass-to-water ratio could be reduced further with process optimization and improved mixing.

Alkali and alkaline earth metal passivation offers a purely thermal route to the production of sugars from lignocellulosic biomass. However, it has previously been demonstrated only with analytical pyrolysis instrumentation using microgram quantities of biomass. The objective of this study is to demonstrate the kilogram scale continuous production of sugar-rich bio-oil from fast pyrolysis of AAEM passivated lignocellulosic biomass.

2. Materials and Methods

2.1. Feedstock Preparation

Northern red oak (*Quercus rubra*) was obtained from Wood Residuals Solutions (Montello, WI). Switchgrass (*Panicum virgatum*) was obtained from Chariton Valley Resource Conservation and Development, Inc. (Centerville, IA). The as-received feedstocks were ground using a Retsch® Type SM2000 Heavy-Duty Cutting Mill with a 750 µm screen, and sieved using a W.S. Tyler Ro-Tap® sieve shaker with screens that allowed separation of the desired size range of 300-710 µm. A portion of the prepared feedstock was set aside as the control and the remainder was AAEM passivated with sulphuric acid.

The required amount of sulphuric acid necessary to passivate the AAEMs in the red oak and switchgrass was calculated using the correlation developed by Kuzhiyil et al.⁷ The red oak and switchgrass were determined to require 0.40 wt. % and 2.0 wt. % sulphuric acid, respectively. Switchgrass required additional sulphuric acid by virtue of its higher AAEM content

The sulphuric acid was first diluted in 18.2 MΩ-cm ultrapure deionized water before it was infused into the feedstocks. Red oak and switchgrass were experimentally determined to be uniformly wetted for mass ratios of biomass-to-water of 1:1 and 1:2, respectively. The dilute acid solutions were prepared using 96.7 wt. % purity sulphuric acid purchased from Fischer Scientific® Accordingly, four kilograms of 0.4 wt. % dilute sulphuric acid solution was required to treat the 4 kg of red oak, while 8 kg of 1.0 wt. % dilute sulphuric acid solution was required to treat the 4 kg of switchgrass.

Biomass and dilute acid were thoroughly mixed by hand in plastic pails until a uniform mixture was achieved. The resulting damp biomass was loaded into shallow plastic bins and dried at 40°C in an oven with an airflow of approximately

five standard litres per minute (SLPM). Once the feedstock was dried to 6-10% moisture content it was removed from the oven and sealed in a clean plastic pail. Actual moisture content of the feedstock was measured just prior to the pyrolysis experiments using a Mettler Toledo TGA/DSC 1®.

2.2. Pyrolysis Experiments

A twin-screw auger reactor was used to conduct laboratory-scale experiments. A diagram of the reactor system is shown in the Supplementary Information.† Further details of the reactor system are described by Brown et al.¹⁵ Shakedown trials with AAEM passivated biomass were used to determine appropriate operating conditions, which were somewhat different from those described by Brown et al.¹⁵ for pyrolysis of untreated biomass (these differences included a higher heat carrier to biomass ratio, lower temperature, and more sweep gas). Biomass and a preheated heat carrier were co-fed into the reactor at 0.25 kg/hr and 10 kg/hr, respectively. The heat carrier consisted of stainless steel cut-wire shot from Pellets LLC (North Tonawanda, New York), which was sieved to a range from 710-1000 µm prior to experiments. Twin screws in the reactor co-rotated at 54 rpm to properly mix the biomass and heat carrier and provide a solids residence time of approximately 10 seconds. The outside of the reactor was heated with a Watlow® ceramic clamshell heater to maintain 550°C. Biomass and heat carrier entered the reactor at 25°C and 550°C, respectively. Heat absorbed by the biomass from the heat carrier during pyrolysis resulted in a reaction temperature near 500°C. A total of 4.0 SLPM of nitrogen was injected into the reactor system as a purge gas using an Alicat® mass flow controller. The pyrolysate and purge gas were discharged from the reactor through a vapour port located 10.8 cm downstream from the heat carrier inlet. The pyrolysate and sweep gas next passed through a cyclone to remove any entrained char before entering the bio-oil collection system.

A cold gas quench system as described by Dalluge et al.¹⁶ was used to quickly quench reaction products leaving the pyrolyzer and recover bio-oil. The pyrolysis vapour stream entered the quench chamber at approximately 500°C and was quenched with the liquid nitrogen to 110°C before entering an electrostatic precipitator (ESP). The bio-oil “heavy ends” collected in the ESP were designated as stage fraction one (SF1). The remaining pyrolysis vapours passed into a shell and tube heat exchanger that maintained a wall temperature of -5°C using a water-ethylene glycol mixture. The bio-oil “light ends” collected in the shell and tube heat exchanger were designated as stage fraction 2 (SF2). Bio-oil fractions were analysed separately; however, results were combined for a whole bio-oil basis in the results and discussion. For each experiment the reactor operated continuously for two hours.

Mass balances were determined by measuring bio-oil, char, and non-condensable gases (NCGs). Total bio-oil yield was calculated by weighing each of the bio-oil collection system components before and after each experiment to determine the total accumulated mass of bio-oil. The mixture of char and heat carrier had to be separated before the char mass could be determined. A majority of the char could be separated from the heat carrier for the untreated biomass by sieving the mixture through a 710 µm screen. Carbon mass percentage in the sieved char was determined via ultimate analysis on a LECO TruSpec® CHNS analyser.

The AAEM passivated biomass lead to agglomerates of char and heat carrier that could not easily be separated.

Therefore, a char burn-off procedure was developed to account for the mass of any char remaining with the heat carrier. The procedure involved loading the char and heat carrier mixture into a fixed bed reactor and heating to 750 °C. Air was purged through the reactor at 4.0 SLPM throughout the procedure in order to oxidize all of the carbon. The burn-off procedure was considered complete when the monitored levels of carbon monoxide and carbon dioxide in the exhaust stream were undetectable. Both the volume and composition of the exhaust stream were recorded and used to determine the total mass of carbon that was combusted from the heat carrier. The calculated carbon mass resulting from carbon monoxide and carbon dioxide in the exhaust stream was then normalized to the percentage of carbon in the sieved char. Both the mass of char from the burn-off procedure and from sieving were added together for the total mass balance.

Non-condensable gases (NCGs) from both the pyrolysis experiments and the char burn-off procedure were quantified by monitoring the concentration of individual gas species and the total volumetric gas flow. Concentrations of NCGs in the exhaust stream were measured using a Varian® CP-4900 micro-Gas Chromatograph (microGC) interfaced with Galaxy® Chromatography software. The microGC was calibrated to quantify helium, hydrogen, oxygen, nitrogen, methane, carbon monoxide, carbon dioxide, ethylene, acetylene, ethane, and propane.

Total exhaust gas volume was measured using a Ritter® TG5/4-ER-1 bar drum type gas meter. The mass of NCGs produced during the reaction was then calculated using the overall gas volume and the steady-state concentrations of NCGs indicated by the microGC.

2.3. Bio-oil Analysis

Bio-oil moisture content was determined using a Karl Fischer MKS-500® moisture titrator. Hydranal Working Medium K® was used as the solvent and Hydranal Composite 5 K® was used as the titrant. The instrument was calibrated using deionized water before analysis.

Cellobiosan (1,6-anhydro-β-D-cellobiose), levoglucosan (1,6-anhydro-β-D-glucopyranose), galactose, and xylosan (1,4-anhydro-α-D-xylopyranose) were quantified via a water wash method followed by analysis with High Performance Liquid Chromatography (HPLC). The water wash method involved dissolving approximately 500 mg of bio-oil in 18.0 mL of DI water. Any water insoluble bio-oil compounds, such as oligosaccharides and lignin oligomers, were removed from the water mixture via centrifugation and filtration prior to analysis.

A Dionex UltiMate® 3000 HPLC system interfaced with Chromeleon® software and a Refractive Index (RI) detector was used to quantify water soluble sugars. Two Bio-Rad® Aminex HPX-87P columns were used in series for sugars separation with a guard column and Micro-guard® cartridge. The column compartment was held at 75°C for analysis. Ultrapure deionized water of 18.2 MΩ-cm purity was used as eluent at a flow rate of 0.6 mL/min. Each sugar was calibrated using a pure standard within the range of 0.5-10 mg/mL using a five point calibration.

Dimeric or oligomeric carbohydrates in bio-oil are difficult to directly quantify. Instead, the saccharides in bio-oil were hydrolysed to glucose, xylose, and sorbitol, which were quantified and combined to give "total sugars." Hydrolysis was accomplished by mixing approximately 60 mg of bio-oil and 6 mL of 400 mM sulphuric acid solution in a reactor vessel. The

vessel was then placed in an oil bath at 125°C for 45 min. The resulting liquid was then filtered and analysed via HPLC.

A Dionex UltiMate® 3000 HPLC system interfaced with Chromeleon® software was used for HPLC analysis. A 300 mm X 7.7 mm 8 μm particle size HyperRez XP Carbohydrate® analytical column was used for separation of the carbohydrates. A Carbohydrate H+® cartridge was used as the guard column prior to the HyperRez XP® column. The mobile phase was 18.2 MΩ-cm deionized water at a flow rate 0.2 mL/min. The column compartment was held isothermally at 55°C. Each sugar was calibrated using a pure standard within the range of 0.5-10 mg/mL using a five point calibration. Further details of the hydrolysis method are available from Johnston and Brown.¹⁷

Water insoluble content, made up of predominately lignin-derived phenolic oligomers, was quantified by mixing bio-oil with 80°C water using a bio-oil-to-water mass ratio of 80:1. The mixture was placed in a 50 mL centrifuge tube and thoroughly mixed using a vortex mixer for one minute. Each centrifuge tube was sonicated for 30 min to ensure proper mixing. Next, the mixture was centrifuged at 2500 rpm for 20 minutes. The supernatant was filtered through a Whatman® size 42 filter (size retention of 2.5 μm) to capture the water insoluble content. Both the centrifuge tube and filter paper were then dried at 50°C for 24 hours. Accumulated mass on both the filter paper and centrifuge tube were considered water insoluble content.

Due to the chemical complexity of the bio-oils, a variety of methods were used to first identify and then quantify bio-oil volatiles. Each method utilized gas chromatography (GC) operating with the same type of column and conditions; however, the detector was alternated between a low resolution Quadrupole Mass Spectrometer (Q-MS), a high resolution Time of Flight Mass Spectrometer (TOF-MS), and a flame ionization detector (FID). The method of Kovats retention index¹⁸ with n-alkanes ranging from C8-C20 was used to estimate retention time changes between each of the three systems.

A 60 m Zebtron ZB-1701® (7KG-G006-11) capillary column with an inner diameter of 0.25 mm, film thickness of 0.25 μm, and a stationary phase of 14% Cyanopropylphenyl and 86% Dimethylpolysiloxane was used for GC analysis. The GC injector operated isothermally at 280°C in split/splitless mode with a split ratio of 20. Ultra high purity helium (99.999%) was used as the carrier gas at a constant flow rate of 2 ml/min through the column. The GC oven was set to first hold at 35°C for 3 minutes, followed by ramping at 2°C/min to 250°C, followed by ramping at 5°C/min to 280°C where it was held for 3 minutes, providing a total run time of 119.5 minutes per sample.

A Varian® 320 Q-MS coupled with a Varian® 450-GC and 8400 autosampler was used for initial peak identification. A volume of 1.0 μL of a 5 wt. % bio-oil solution in methanol was injected on the GC for peak identification samples. The mass spectrometer operated in negative electron ionization mode (EI (-)). The source temperature was set at 280°C. The filament operated at -70 eV and an emission current of 68.75 μA. The detector scanned in the range of 30-650 Da at a rate of 2 scans per second. The 2008 NIST library was used to identify several of the compounds, whereas compounds that were not identified, or had a low probability, were compared to literature for most likely match.^{19, 20} Several compounds were not identifiable via Q-MS due to the fragmentation experienced using EI (-), therefore the TOF-MS was used to determine molecular formula of several previously unknown compounds.

A GCT® GC-MS that is an orthogonal TOF-MS from Waters Inc., Milford, MA was used to acquire accurate mass data (GC-TOF). The system utilized a model 6890 GC from Agilent®, Santa Clara, CA, which is equipped with a model 7683 Autoinjector also from Agilent®. The GC-TOF operated in positive chemical ionization mode (CI(+)) utilizing ammonia dopant gas in attempt to identify molecular ions without fragmentation. The source temperature was set to 120°C and operated at 30 eV and 200 µA. The detector scanned in the range of 35-650 Da at a rate of 2 scans per second. The MS achieved a resolution near 7000. Accurate mass data was acquired using a calibrant of chloropentafluorobenzene with an exact mass of 201.9609 Da.

A Bruker® 430-GC with a Varian® CP-8400 liquid injection autosampler interfaced with Galaxy® software was used for GC-FID analysis. The FID was set at 300°C with 25 mL/min helium makeup flow, 30 mL/min hydrogen, and 300 mL/min air flow. Calibration was performed using the method outlined by de Saint Laumer et al.²¹ A four point calibration was first attained using methyl octanoate as a standard. The relative response factor of each individual compound was calculated using the enthalpy of combustion outlined in equations 5, 10, and 15 in the de Saint Laumer et al. paper.²¹ The area response for each peak was first normalized to the response of methyl octanoate and then multiplied by the relative response factor for each compound. Several bio-oil compounds were injected at known concentrations and compared to the theoretical yield obtained using the response factors with good correlation.

A Dionex® ICS3000 ion chromatography system with a conductivity detector and an Anion Micromembrane Suppressor (AMMS-ICE 300®) was used for organic acids analysis. The Dionex® system was interfaced with Chromeleon® software version 6.8. Tetrabutylammonium hydroxide in water at a concentration of 5 mM was used to regenerate the suppressor at a flow rate of 4-5 mL/min. A mixture of 1.0 mM heptafluorobutyric acid in water was used for the eluent at a flow rate of 0.120 mL/min at 19°C. An IonPac® ICE-AS1 4x50 mm guard column in series with an IonPac® ICE-AS1 4x250 mm analytical column were used for separation. Standards of acetate, propionate, formate and glycolate were purchased from Inorganic Ventures to calibrate the instrument. The concentrated standard was certified at 200.0 ± 1.3 mg/L for all acids and was diluted down with 18.2 Ω-cm ultrapure deionized water to concentrations of 10.0, 25.0, 67.0, 100.0, and 200.0 mg/L to achieve a five point linear calibration.

Mass closure from each of the subsequent bio-oil analyses accounted for 68.8 wt. %, 82.2 wt. %, 72.3 wt. %, and 76.7 wt. % of the total bio-oil, respectively, for red oak, AAEM passivated red oak, switchgrass and AAEM passivated switchgrass. The remaining 20-30% of the bio-oil mass that could not be accounted for with the subsequent analysis likely consists of unhydrolyzable carbohydrates and components that are not in sufficient concentration to quantify on their own. Pyrolysis experiments were performed in duplicate for each feedstock. Error bars in the subsequent figures indicate standard deviation of the trials. The Student T-test was used to compare the mean value from each treatment and the p-values are reported in the Supplementary Information.† A p-value less than 0.05 indicates a statistically significant difference at a 95% confidence interval, whereas a p-value of 0.10 or less indicates a statistically significant difference in the means at a 90% confidence interval, and so on.

3. Results and Discussion

3.1. Liquid Products

3.1.1. Anhydrosugars

Anhydrosugars from pyrolysis of AAEM passivated feedstock significantly increased for both red oak and switchgrass, both at 95% confidence. As shown in Figure 1, the sugar yield from AAEM passivated red oak increased by 180% compared to the control. Similarly with AAEM passivated switchgrass the sugar yield increased by 198% compared to the control. All individual anhydrosugars except for xyloosan increased significantly with AAEM passivation. Levoglucosan increased the most significantly as a result of AAEM passivation, increasing by 316% for red oak and 388% for switchgrass.

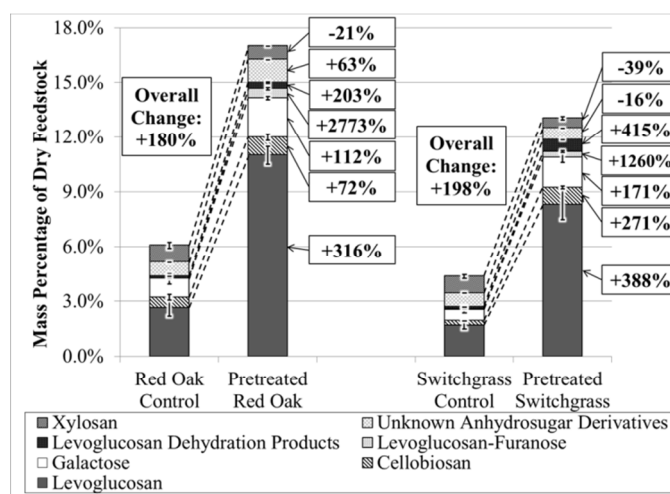


Figure 1: Mono- and disaccharide yield from control and AAEM passivated feedstocks.

Compounds labelled as levoglucosan dehydration products consisted of 1,4:3,6-dianhydro- α -D-glucopyranose (singly dehydrated levoglucosan) and levoglucosenone (doubly dehydrated levoglucosan). Levoglucosan dehydration products from red oak approximately tripled as a result of AAEM passivation. For AAEM passivated switchgrass the increase was over five-fold. Although both 1,4:3,6-dianhydro- α -D-glucopyranose and levoglucosenone are generally low in yield, they derive from the dehydration of levoglucosan, giving some indication as to the fate of carbohydrates during pyrolysis.²² The increase in levoglucosan dehydration products is likely due to the presence of the infused acid, which can catalyse dehydration of carbohydrate during pyrolysis. The more dramatic increase in levoglucosan dehydration products for switchgrass correlates with an increased amount of acid used for its passivation.

Mass spectra of the compounds labelled as “unknown anhydrosugar derivatives” suggests that they have similar structure to other anhydrosugars; however, their molecular formula found via GC-TOF was not consistent with conventional anhydrosugars. Unknown anhydrosugar derivatives increased slightly with AAEM passivation of red oak and slightly decreased for switchgrass. The molecular formula of the unknown anhydrosugar derivatives was found from the molecular ion via GC-TOF. The molecular formulas suggest these may be glycosides with various functionality

attached to an anhydrosugar backbone; similar to those found by Smith et al.²³ However, detailed structural analysis of the unknown anhydrosugar derivatives is outside the scope of this paper. The molecular formula of each compound found using GC-TOF is available in the Supplementary Information.† Each of the unknown anhydrosugar derivatives is labelled as a “carbohydrate derivative” numbered between 2-16. It should be noted that several unknown peaks appeared in HPLC analysis that were not quantified, which are likely some of the unidentified anhydrosugars found via GC analysis.

3.1.2. Total Sugars

Bio-oil carbohydrates were hydrolysed to isomers of glucose, xylose, or sorbitol for the purpose of determining total sugar content. In this section the sugars are labelled by their hydrolysis products; e.g. all saccharides that are hydrolysed to glucose are termed “glucose hydrolysable sugars.” The sum of all the glucose, xylose, and sorbitol hydrolysable sugars is termed “total sugars.” As shown in Figure 2, the yield of total sugars increased by 105% as a result of AAEM passivation for red oak and increased by a remarkable 259% for switchgrass.

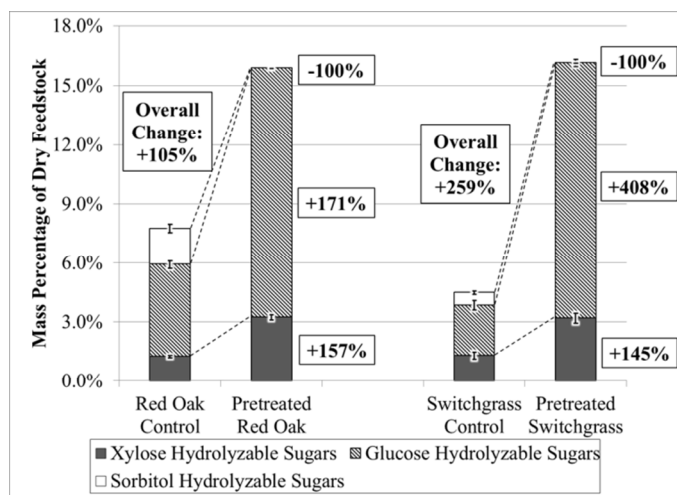


Figure 2: Total sugar yields from control and AAEM passivated feedstocks.

Sorbitol was completely eliminated as a result of AAEM passivation. Sorbitol, a sugar alcohol, is the most highly hydrated of the analysed sugars. The presence of acid from the AAEM passivation process likely prevented formation of the more hydrated compounds, thus decreasing the yield of sorbitol hydrolysable sugars.

Glucose hydrolysable sugars accounted for the largest increase in sugars. The increase in glucose hydrolysable sugars as a result of AAEM passivation of switchgrass is similar to the increase in levoglucosan, as might be expected. For red oak the yield of levoglucosan increased by 316%, whereas glucose hydrolysable sugars increased by only 171%. This large discrepancy suggests that a significant portion of the glucose hydrolysable sugars from untreated red oak are derived from compounds other than levoglucosan, possibly oligosaccharides or some of the unknown anhydrosugar derivatives.

Xylose hydrolysable sugars increased by nearly 150% for pyrolysis of both red oak and switchgrass as a result of AAEM passivation. The yield of the anhydrosugar precursor xylosan however decreased for each feedstock. The increase in xylose

hydrolysable sugars suggests that AAEM passivation is effective in increasing yield of pentoses and pentosans from hemicellulose. Several of the individual pentosans in bio-oil have not been identified or quantified. These unknown pentosans likely make up the xylose hydrolysable sugars that are not accounted for via xylosan.

The overall yield of sugars accounted for via HPLC and GC analysis was slightly higher than the yield of total sugars measured via hydrolysis. The difference in quantity of anhydrosugars and hydrolysable sugars suggests that several of the anhydrosugars might not be readily hydrolysable to glucose, xylose, or sorbitol.

3.1.3. Carbohydrate Dehydration Products

Products of carbohydrate dehydration include furans, tetrahydrofurans, lactones, cyclopentanes, pyrans, and miscellaneous furanoids. Each compound classification was categorized into the carbohydrate dehydration products (CDPs) group since each of them have a higher carbon-to-oxygen ratio than anhydrosugars, but do not contain benzene rings typical of lignin products. As shown in Figure 3, overall CDPs decreased with AAEM passivation, which was the case for all classifications except furans. This is somewhat surprising as acid catalysed dehydration of carbohydrates as a result of the addition of acid during the AAEM passivation process is expected to increase CDPs, as was the case for furans. Therefore, it is likely that several of the CDPs are formed from reactions other than carbohydrate dehydration.

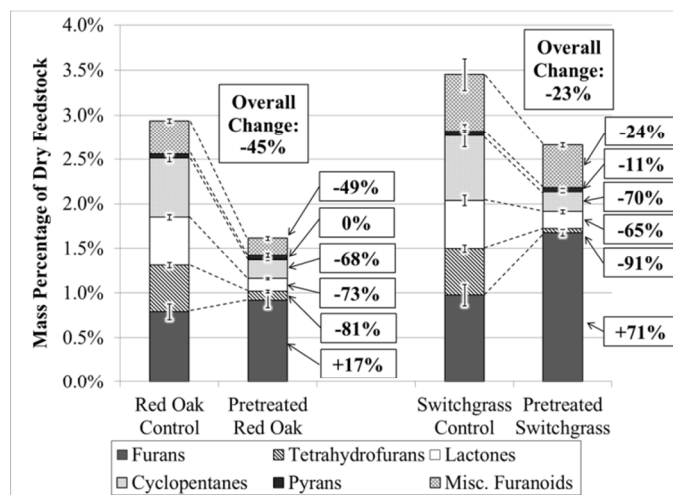


Figure 3: Carbohydrate dehydration product yields from control and AAEM passivated feedstocks.

Cyclopentanes decreased by nearly 70% for each AAEM passivated feedstock. Cyclopentanes have been identified by many researchers; however, to our knowledge their formation has not been investigated in detail. Lack of research on cyclopentanes is most likely due to their low yield of typically less than 1 wt. % of the original biomass. Cyclopentanes have been investigated more extensively in the flavour and fragrance industry²⁴ and in the roasting of coffee.²⁵ Because anhydrosugars have limited vapour pressure²⁶ and no odour, compounds such as cyclopentanes and lactones are likely major contributors to the typically sweet smell of bio-oil carbohydrates.

Cyclopentanes have been observed to form in the condensed phase by several researchers. Shaw et al.²⁷ found cyclopentanes and lactones to be produced in the acid catalysed degradation of carbohydrates in an aqueous phase, which may be a source of carbohydrate degradation commonly observed in bio-oil aging. Niemela et al.²⁸ observed cyclopentanes to result from the condensation of light oxygenate precursors through aldol-condensation reactions, which also occurred in the condensed phase. The products from AAEM passivated feedstocks would be expected to show increased cyclopentanes as a result of acid catalysed dehydration if, in fact, cyclopentanes were primary products resulting from dehydration during pyrolysis. However, cyclopentanes decreased as a result of AAEM passivation and the decrease directly correlated to a decrease in light oxygenates. Therefore, it is likely that cyclopentanes are secondary products resulting from condensation of light oxygenates in the condensed bio-oil.

Similar to cyclopentanes, lactones decreased by nearly 70% from both AAEM passivated feedstocks. It is likely that, similar to cyclopentanes, lactones are formed via condensation reactions of light oxygenates in the bio-oil as was found by Niemela et al.²⁸

Tetrahydrofurans from passivated feedstock decreased substantially. The decrease was 81% (for red oak and 91% for switchgrass. To our knowledge, no mechanism has been proposed for the direct production of tetrahydrofurans from biomass pyrolysis. The saturated furan ring is unlikely to be formed from carbohydrates as the elimination of hydroxyl groups from the furan moiety in carbohydrate dehydration would more likely produce unsaturated furan moieties. Similar to cyclopentanes and lactones, the tetrahydrofurans are likely formed via secondary condensation of light oxygenates in the bio-oil.

Furans increased by 16% for AAEM passivated red oak and 70% for AAEM passivated switchgrass. Furans, especially furfural and 5-(hydroxymethyl)furfural, are known to be products of carbohydrate dehydration.^{4, 29-31} The more significant increase observed for switchgrass is likely due to the increased amount of acid used to passivate its AAEM content.²⁹ The increase in furans from AAEM passivated feedstock is consistent with observations of Kuzhiyil et al.⁷ and with those of several others investigating different methods of using acid to increase sugar yields.^{14, 32}

The group labelled “miscellaneous furanoids” consists of compounds that were not structurally identified; however, they have molecular formulas and fragmentation patterns similar to furans, lactones, or cyclopentanes. The compound labelled in the Supplementary Information† as “furan derivative 16A” was the most dominant of the unknown furanoids, yielding as much as 0.5 wt. % from pyrolysis of the untreated switchgrass. Alkali and alkaline earth metal passivation reduced miscellaneous furanoids from 0.28 wt. % to 0.13 wt. % of feedstock from red oak and from 0.49 wt. % to 0.32 wt. % of feedstock from switchgrass. Like all CDPs (except furans) miscellaneous furanoids decreased with AAEM passivation. Miscellaneous furanoids are therefore likely cyclopentanes, lactones, or tetrahydrofurans as opposed to simple furan derivatives.

3.1.4. Lignin Products

Alkali and alkaline earth metal passivated feedstocks produced less water insoluble lignin oligomers, also known as pyrolytic lignin. As shown in Figure 4, lignin oligomers from

AAEM passivated red oak decreased by 49%. Switchgrass showed a similar trend decreasing from 9.0 wt. % to 7.7 wt. % of feedstock, although the decrease was not significant at the 90% confidence interval. Mass yields of volatile lignin-derived products are shown in Figure 5. Phenolic compounds containing no methoxyl side chains decreased by 54% from AAEM passivated red oak. Total phenolic compounds from switchgrass decreased by 63%.

Guaiacols, containing one methoxyl side chain, decreased by 45% from AAEM passivated red oak and decreased by 36% for switchgrass. Guaiacols with unsaturated side chains such as eugenol, isoeugenol, and methyleugenol, decreased most dramatically, to near undetectable levels in bio-oil from AAEM passivated feedstock.

Syringols, containing two methoxyl side chains, decreased by 67% from AAEM passivated red oak. Switchgrass showed a similar trend with a decrease of 42%. Similar to guaiacols, syringols with unsaturated side chains such as 2,6-dimethoxy-4-vinylphenol, 4-(2-propenyl)-2,6-dimethoxyphenol, and 4-(1-propenyl)-2,6-dimethoxyphenol decreased significantly.

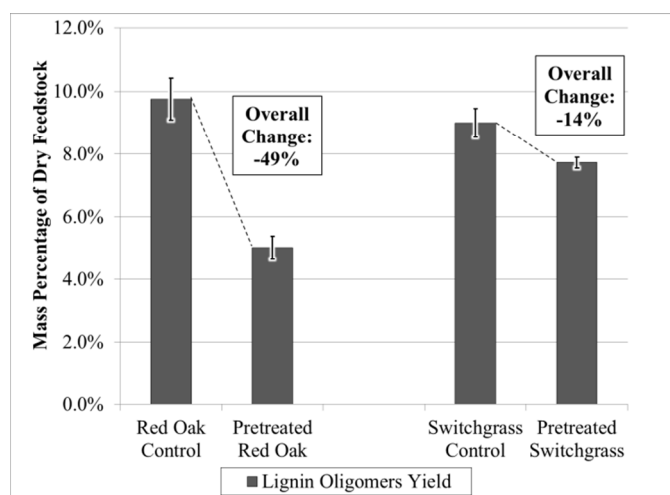


Figure 4: Lignin oligomer yields from control and AAEM passivated feedstocks.

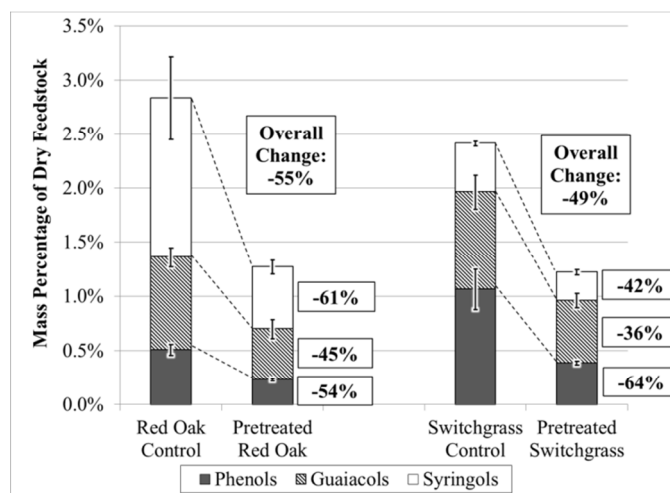


Figure 5: Volatile lignin product yields from control and AAEM passivated feedstocks.

Total phenolic compounds decreased more from red oak than switchgrass as a result of AAEM passivation. Red oak, a

hardwood, is known to contain more S-lignin compared to switchgrass.³³ The decrease in red oak lignin products is therefore consistent with the observation of Asmadi et al.³⁴ who found S-lignin to be more reactive in secondary polymerization and coking reactions than G-lignin. Asmadi et al.³⁴ found the methoxyl side chains of guaiacol and syringol to undergo homolysis and rearrangement at temperatures as low as 400–450°C; well below the pyrolysis temperatures used in this work. Homolysis of ether bonds from both the guaiacol and syringol moieties at low temperatures produces highly reactive radicals that then can polymerize to produce char and phenolic oligomers. In another study Asmadi et al.³⁵ found that the reactivity of phenolic monomers generally increased with increasing numbers of substituents groups. Compounds from S-lignin have the highest number of substituents per benzene moiety, making them the most reactive.

In contrast, Mullen et al.³⁶ found recombination reactions of S-lignin to be less reactive when comparing pyrolysis of red oak and barley hulls. Scholze et al.³⁷ also found conflicting results and attributed the higher reactivity of G-lignin to the open C5 position on guaiacol moieties, which is prone to condensation reactions. Conflicting results may indicate that several mechanisms are responsible for the formation of char and phenolic oligomers from lignin. Mechanisms involving the quinone methide intermediate, as suggested by Hosoya et al.,^{38, 39} would lead to bond formation on the methide side chain. A reaction involving the open C5 position on guaiacol moieties, as suggested by Scholze et al.,³⁷ would more likely form bonds directly on the aromatic ring. Therefore, in addition to the methoxy groups on the lignin moieties, the linkage type and proximity to constituents capable of cross-linking likely plays a role in char formation. A more detailed analysis of char and phenolic oligomer structure would need to be performed in order to determine the most important mechanisms in their formation.

3.1.5. Light Oxygenates

As shown in Figure 6, light aldehydes decreased by 56% for red oak and by 32% for switchgrass as a result of AAEM passivation. Acetaldehyde and glycolaldehyde are the only two aldehydes which were quantified in this work, although several other aldehydes including formaldehyde and larger aldehydes have been observed by other researchers to be products of AAEM catalysed fragmentation of glucose rings.^{4, 6, 8, 40} The decrease in aldehydes is indicative of less pyranose and furanose ring fragmentation from holocellulose pyrolysis as a result of AAEM passivation.

Aldehydes are known to undergo polymerization and condensation reactions such as aldol condensation and Diels-Alder cyclization reactions, both of which are catalysed by acids. The mixture of aldehydes, alcohols, and carboxylic acids in bio-oil make it very unstable, promoting polymerization to resinous material.⁴¹ Glycolaldehyde itself is so reactive toward polymerization, even with itself, that the monomer is not available for purchase as a calibration standard. Therefore, glycolaldehyde could only be confirmed via mass spec and quantified via theoretical response factors. Glycolaldehyde, nonetheless, is commonly reported in bio-oils. Due to its reactivity toward polymerization it is doubtful that glycolaldehyde is a constituent of bio-oil and is more likely a degradation product of unstable bio-oil components during analysis. To our knowledge glycolaldehyde is always quantified via GC, meaning that the bio-oil is first subject to a high

temperature injector. Semi-stable intermediates, such as those found by Smith et al.²³, exposed to high injector temperatures are likely to decompose and form glycolaldehyde and other fragmentation products. Therefore, glycolaldehyde is likely a product of secondary decomposition of semi-stable intermediates in bio-oil during analysis, rather than present in the condensed bio-oil. Regardless, the decrease in aldehydes is expected to lead to more stable bio-oil.

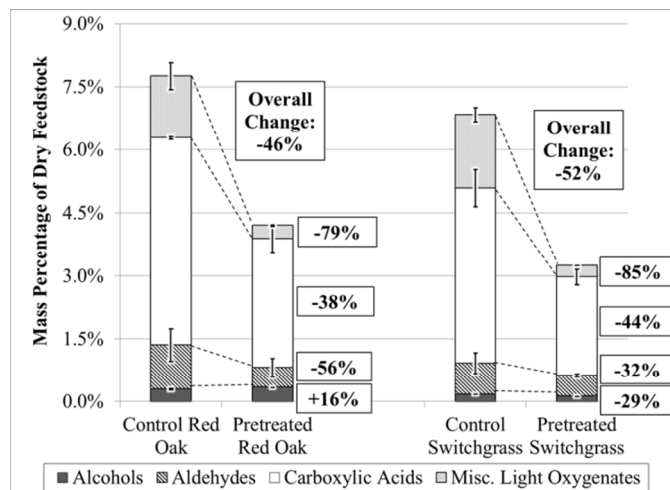


Figure 6: Light oxygenates yield from control and AAEM passivated feedstocks.

Carboxylic acids in bio-oil from AAEM passivated feedstock decreased by 29% for red oak and by 44% for switchgrass. Carboxylic acids, especially acetic acid, are known to form from thermal decomposition products from all three biomass constituents, with the majority of fragmented acetyl groups coming from pentosans in the hemicellulose.^{42, 43}

The category labelled “miscellaneous light oxygenates” consists of primarily light ketones with hydroxyacetone making up the majority of this category. Miscellaneous light oxygenates decreased by 79% for red oak and by 85% for switchgrass as a result of AAEM passivation. Anything categorized as miscellaneous light oxygenates is thought to come from fragmentation of carbohydrates. Therefore, the observed decrease in miscellaneous light oxygenates suggests reduced fragmentation of biomass carbohydrates for AAEM passivated feedstocks.

3.1.6. Reaction Water

Reaction water was calculated by first determining the total mass of water in the bio-oil using Karl Fischer titration followed by subtracting the mass of water that was contributed from moisture in the incoming feedstock. As shown in Figure 7, the reaction water increased for AAEM passivated feedstocks. The increase in water correlates with an increase in char as might be expected as both are products of biomass carbonization.⁴⁴ Of course, other acid-catalysed dehydration processes also contribute to the observed increase in product water.

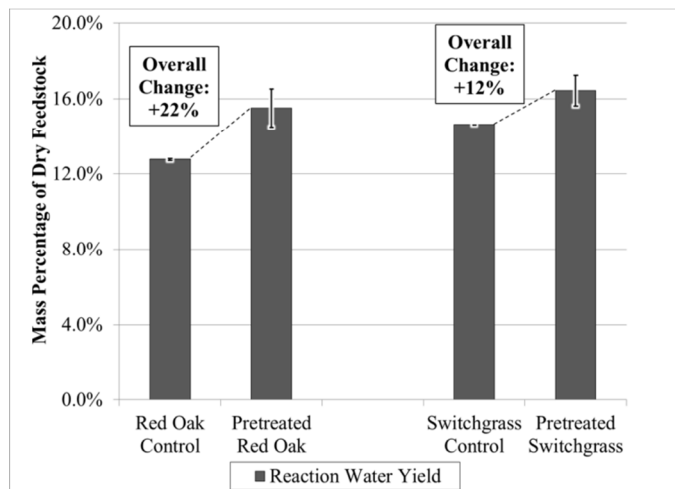


Figure 7: Reaction water yield from control and AAEM passivated feedstocks.

3.2. Char

Chars produced from AAEM passivated feedstocks had different physical properties than chars produced from untreated material. Chars produced from each of the control feedstocks were observed to be similar in size to the original biomass although black in colour and more porous. Char produced from AAEM passivated red oak ranges in size from fine powder to large agglomerates that encapsulated some of the heat carrier, as shown in Figure 8. Char from AAEM passivated switchgrass also contained both fine powder and agglomerates although large agglomerates were not as prevalent. Chars from both AAEM passivated feedstocks took on a vitreous lustre and appeared as if they had been in a molten state before charring. The finer material is likely the product of agglomerates being mechanically pulverized as they were conveyed through the auger reactor.



Figure 8: Large char agglomerate resulting from fast pyrolysis of AAEM passivated red oak.

Agglomerated material was difficult to separate from the heat carrier. Prior to pyrolysis, feedstock was sieved to pass a 710 μm screen whereas heat carrier material was sieved to eliminate all particles below 710 μm . Thus, in the absence of agglomeration, char particles would be expected to be smaller than the heat carrier. As shown in Figure 9, over 95 wt. % of the char was separated from the heat carrier by sieving for each of the control feedstocks and only 5 wt. % of the char had to be burned from the heat carrier. In contrast, for pyrolysis of

AAEM passivated red oak only about 10 wt. % of the char was recovered by sieving while 90 wt. % of the char had to be removed via the char burn-off procedure. For pyrolysis of AAEM passivated switchgrass, fine and agglomerated char were present in approximately equal amounts. The large increase in char production from pyrolysis of AAEM passivated feedstocks and the different character of this char compared to the control chars suggests a different mechanism for its formation during pyrolysis.

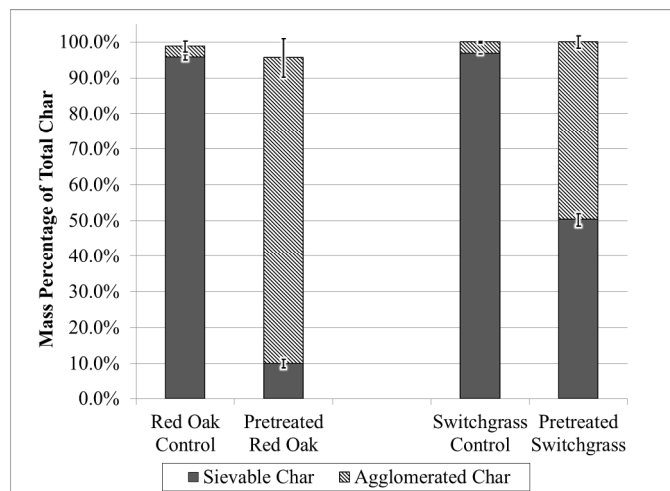


Figure 9: Char separation comparison for control and AAEM passivated feedstocks.

Char increased by 9.5 wt. % and 6.4 wt. % for AAEM passivated red oak and switchgrass, respectively. Lignin-derived phenolic compounds decreased by 6.4 wt. % and 2.4 wt. % for these same pretreated feedstocks. Thus, assuming the entirety of the decrease in phenolic compounds is converted to char; acid-catalysed dehydration of phenolic compounds can explain 67% and 38% of increased char production for AAEM passivated red oak and switchgrass, respectively.

The larger conversion of phenolic compounds to char for red oak compared to switchgrass may be the result of the higher methoxyl content for this feedstock. Methoxyl side chains are known to promote secondary polymerization and coking reactions during lignin pyrolysis.^{34,45} Hosoya et al.³⁸ postulated a mechanism for the formation of char from methoxyl side chains in lignin where electron donating properties of the methoxyl side chain contributed to its higher reactivity. The reaction is thought to be initiated by H-atom abstraction from the phenolic hydroxyl group followed by rearrangement and dehydration within the aromatic ring to form an o-quinone methide intermediate. Zhou et al.⁴⁵ found char yields from fast pyrolysis of Douglas fir, which contains high levels of G-lignin, to increase after pretreatment with sulphuric acid. Zhout et al.⁴⁵ postulated that sulphuric acid catalyses the dehydration step in the mechanism described by Hosoya et al. Red oak, being a hardwood, contains many more methoxyl side chains than the lignin in switchgrass. Therefore, the increased lignin-derived char from red oak can be explained by the additional methoxyl side chains of the S-lignin in red oak compared to the H-lignin of switchgrass.

The remaining 33% char increase for AAEM passivated red oak (3.1 wt. % char) and 62% char increase for switchgrass (4.0 wt. % char) must arise from increased carbonization of carbohydrate. Kuzhiyil et al.⁷ found that micropyrolysis trials of AAEM passivated red oak and switchgrass produced

23.4 wt. % and 15.4 wt. % levoglucosan, respectively. Although red oak and switchgrass used in the present study were AAEM passivated in the same manner, the levoglucosan yields were more modest: 11.0 wt. % for AAEM passivated red oak and 8.3 wt. % for AAEM passivated switchgrass. The differences between these two studies might be attributed to enhanced carbonization of levoglucosan in the continuous reactor employed in the present study to form char. Complete carbonization of 1 mol of levoglucosan would produce 6 mol of char, a mass yield of 42 wt. %. Thus, the observed deficit of levoglucosan in the continuous trials of 12.4 wt. % for AAEM passivated red oak and 7.1 wt. % for AAEM passivated switchgrass might be accounted for as additional char production in the amounts of 5.2 wt. % and 2.9 wt. %, respectively. These are close to the amounts of “carbohydrate-derived” char observed.

Enhanced carbonization of levoglucosan released during pyrolysis of acid-infused biomass can be expected under mass transfer limited reaction conditions. The relatively low vapour pressure of levoglucosan results in competing processes of volatilization and oligomerization of levoglucosan.⁴⁶⁻⁴⁸ Carbohydrate oligomers formed from polymerization of levoglucosan are susceptible to dehydration and char formation. Carbohydrate oligomers, being less likely to volatilize, would instead remain in the reactor and eventually dehydrate to char. These carbohydrate oligomers might also hinder the escape of phenolic oligomers released during pyrolysis of the lignin in biomass, enhancing their polymerization and charring. Increased reaction water from AAEM passivated feedstocks is a likely indicator of increased dehydration reactions associated with char formation.

Mass transfer limitations are more likely with the continuous reactor employed in the present study than the micro-pyrolyzer used by Kuzhiyil et al.⁷ Micro-pyrolyzers are designed to operate with very small biomass samples in high volumetric flow rates of sweep gas to avoid mass transfer limitations. The auger reactor was designed to operate at low sweep gas volumetric flows.

Another possible source of increased carbohydrate-derived char is caramelization of sugars during pyrolysis. Caramelization has been shown to produce both light compounds such as furans and heavy compounds referred to as caramelans, caramelens, and caramelins.⁴⁹⁻⁵¹ Hodge et al.⁵² found enolization and dehydration steps associated with caramelization to be catalysed by acids and acid salts. Caramelization reactions during pyrolysis of AAEM passivated feedstocks would likely be catalysed by acid salts formed during the passivation process. Caramelized products would be relatively non-volatile and therefore remain in the reactor, eventually dehydrating to char.

Acid catalysed caramelization of carbohydrates can also explain the different yields of carbohydrate-derived char from red oak and switchgrass. Assuming the entire decrease in lignin-derived products resulted in char, the remaining 3.1 wt. % and 4.0 wt. % char from red oak and switchgrass, respectively, would be carbohydrate derived. Switchgrass had a much higher level of AAEMs and required more sulphuric acid for AAEM passivation (0.4 wt. % acid for red oak versus 2.0 wt. % acid for switchgrass). Acid salts produced from AAEM passivation would be more prevalent in switchgrass than in red oak. Increasing amounts of acid salts likely result in increased acid catalysed caramelization and dehydration of carbohydrates during pyrolysis. Furans, known to result from both caramelization and dehydration of carbohydrates, increased

more significantly for switchgrass than red oak (71% increase for switchgrass versus 16% increase for red oak). The increase in furans is another likely indicator of increased caramelization and dehydration with additional acid salts. Along with furans, increased caramelization would also result in increased carbohydrate oligomers. Unable to volatilize in the pyrolyzer, they would eventually dehydrate to char. The abundance of acid salts in the acid-infused biomass would be expected to contribute to increased carbohydrate-derived char.

3.3. Non-condensable Gases

As shown in Figure 10, non-condensable gases (NCGs) decreased by 46% from both red oak and switchgrass as a result of AAEM passivation. There were no discernable trends in individual gas yields, as carbon monoxide, carbon dioxide, and light hydrocarbons show similar decreases. Figure 6 shows overall light oxygenates to also decrease by 46% and 52% for red oak and switchgrass, respectively, as a result of AAEM passivation. The decrease in NCGs directly correlates with a decrease in light oxygenates, suggesting light oxygenates and NCGs are co-products, as described by Patwardhan et al.⁶ The sum of NCGs and light oxygenates decreased by 12.4 wt. % for red oak and 9.5 wt. % for switchgrass. The sugar yield increased by 8.1 wt. % for red oak and 11.7 wt. % for switchgrass. The decrease in light oxygenates is inversely proportional to the increase in sugars, further supporting the hypothesis that AAEM passivation preferentially increases depolymerization of holocellulose and decreases sugar motif fragmentation. Hence, it would be expected that light oxygenates and NCGs would decrease as sugars increase since they are formed from the same material.

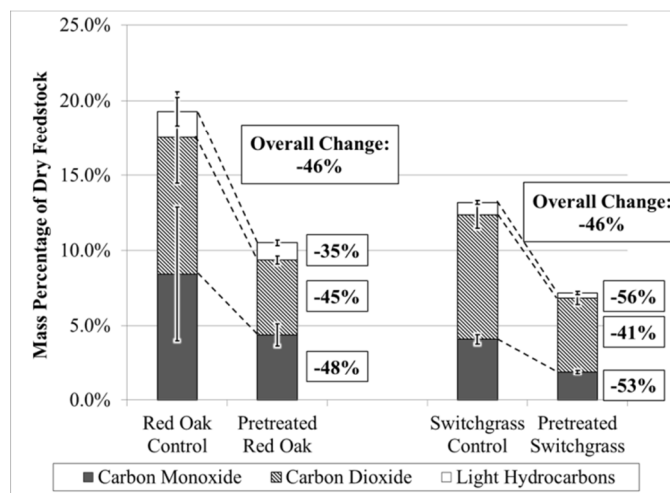


Figure 10: Non-condensable gas yields from control and AAEM passivated feedstocks.

3.4. Overall Mass Yields of Bio-oil, Char, and Gas

As shown in Figure 11, mass closure for each of the experimental sets was near 90 wt. %. Alkali and alkaline earth metal passivation lead to an overall decrease in non-condensable gases and an increase in char. Total bio-oil yield decreased for AAEM passivated red oak and slightly increased for AAEM passivated switchgrass. The decrease in bio-oil for red oak, however, coincided with the maximum sugar yield.

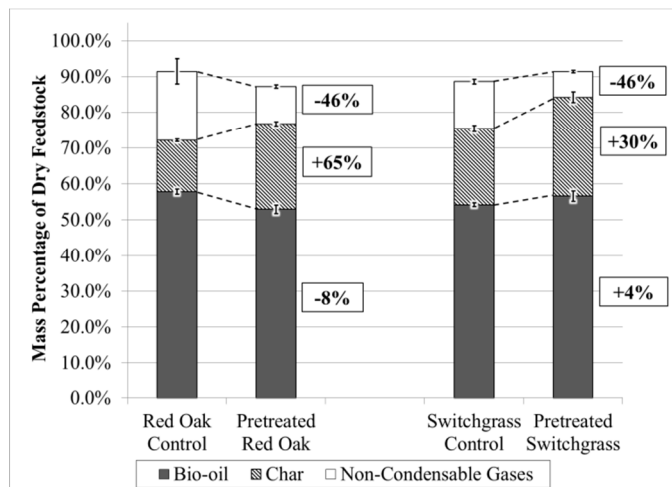


Figure 11: Mass balance comparison for control and AAEM passivated feedstocks.

4. Conclusions

Alkali and alkaline earth metal passivation of red oak and switchgrass prior to pyrolysis was shown to substantially increase total sugar yield in a continuous, lab-scale auger pyrolyzer. Light oxygenates and non-condensable gases decreased in direct proportion to the increase in sugars. The combined increase in anhydrosugar yield and decrease in light oxygenates yield supports the hypothesis that AAEM passivation enhances glycosidic bond cleavage as opposed to pyranose and furanose ring scission of plant polysaccharides. Char increased with AAEM passivation for both feedstocks compared to their controls. Assuming all of the decrease in lignin derived products carbonizes to char, alkali and alkaline earth metal passivated red oak appears to produce more lignin-derived char, whereas AAEM passivated switchgrass appears to produce more carbohydrate-derived char. The higher S-lignin content of red oak compared to switchgrass explains its enhanced lignin-derived char formation when AAEM passivated. Acid catalysed caramelization of carbohydrates is hypothesized to play a role in the enhanced formation of carbohydrate-derived char. This study demonstrates the potential for continuous, non-enzymatic sugar production from the pyrolysis of acid-infused lignocellulosic biomass.

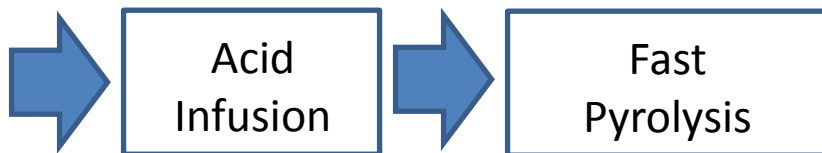
Acknowledgements

We gratefully acknowledge generous funding from the Phillips 66 Company and the U.S. Department of Energy. The authors appreciate the assistance of Nate Hamlett, Emily Hansen, Nick Miller, Jordan Donner, William Paisley, and Nicholas Jaegers in running pyrolysis experiments and preparing samples for analysis. We would like to thank Ryan Smith and Marjorie Rover for their help in many aspects of this project. We also thank Dr. Max Morris for discussions on statistical analysis of the results. We appreciate the assistance of Dr. Steve Vessey at the Chemical Instrumentation Facility at Iowa State University for training and assistance pertaining to the Waters GC-TOF results included in this publication.

Notes and references

- ^a Department of Mechanical Engineering, Iowa State University, 2025 Black Engineering, Ames, Iowa 50011
- ^b Center for Sustainable Environmental Technologies, Iowa State University, 1140 Biorenewables Research Laboratory, Ames, Iowa 50011
- † Electronic Supplementary Information (ESI) available: Auger Reactor Diagram. Individual compound summary for control and AAEM passivated red oak. Individual compound summary for control and AAEM passivated switchgrass. See DOI: 10.1039/b000000x/
1. J. R. Regalbuto, *Science*, 2009, **325**, 822-824.
2. G. W. Huber, S. Iborra and A. Corma, *Chemical Reviews*, 2006, **106**, 4044-4098.
3. F. Shafizadeh, R. H. Furneaux, T. G. Cochran, J. P. Scholl and Y. Sakai, *Journal of Applied Polymer Science*, 1979, **23**, 3525-3539.
4. P. R. Patwardhan, J. A. Satrio, R. C. Brown and B. H. Shanks, *Journal of Analytical and Applied Pyrolysis*, 2009, **86**, 323-330.
5. J. Piskorz, D. S. A. G. Radlein, D. S. Scott and S. Czernik, *Journal of Analytical and Applied Pyrolysis*, 1989, **16**, 127-142.
6. P. R. Patwardhan, J. A. Satrio, R. C. Brown and B. H. Shanks, *Bioresource Technology*, 2010, **101**, 4646-4655.
7. N. Kuzhiyil, D. Dalluge, X. Bai, K. H. Kim and R. C. Brown, *ChemSusChem*, 2012, **5**, 2228-2236.
8. C.-y. Yang, X.-s. Lu, W.-g. Lin, X.-m. Yang and J.-z. Yao, *Chemical Research in Chinese Universities*, 2006, **22**, 524-532.
9. S. Zhou, D. Mourant, C. Lievens, Y. Wang, C.-Z. Li and M. Garcia-Perez, *Fuel*, 2013, **104**, 536-546.
10. R. C. Brown, D. Radlein and J. Piskorz, in *Chemicals and Materials from Renewable Resources*, American Chemical Society, 2001, pp. 123-132.
11. E. B. Hassan, H. Abou-Yousef and P. Steele, *Fuel Processing Technology*, 2013, **110**, 65-72.
12. D. S. Scott, L. Paterson, J. Piskorz and D. Radlein, *Journal of Analytical and Applied Pyrolysis*, 2001, **57**, 169-176.
13. S. Oudenhoven, R. Westerhof, N. Aldenkamp, D. Brilman and S. Kersten, *Journal of Analytical and Applied Pyrolysis*, 2012.
14. C. Di Blasi, C. Branca and A. Galgano, *Polymer Degradation and Stability*, 2008, **93**, 335-346.
15. J. N. Brown, Iowa State University, Ames, Iowa, 2009.
16. D. L. Dalluge, Y. S. Choi, B. H. Shanks and R. C. Brown, *Manuscript submitted for publication (copy on file with author)*, 2013.
17. P. A. Johnston and R. C. Brown, *Analytical Chemistry*, 2013.
18. E. Kováts, *Helvetica Chimica Acta*, 1958, **41**, 1915-1932.
19. O. Faix, I. Fortmann, J. Bremer and D. Meier, *Holz als Roh-und Werkstoff*, 1991, **49**, 299-304.
20. O. Faix, D. Meier and I. Fortmann, *Holz als Roh-und Werkstoff*, 1990, **48**, 351-354.
21. J.-Y. de Saint Laumer, E. Cicchetti, P. Merle, J. Egger and A. Chaintreau, *Analytical Chemistry*, 2010, **82**, 6457-6462.
22. M. R. Nimlos and R. J. Evans, *Fuel Chem Div Prepr*, 2002, **47**, 393-394.
23. E. Smith, C. Hutchinson, D. P. Cole and Y.-J. Lee, in *61st ASMS Conference on Mass Spectrometry and Allied Topics*, Minneapolis, Minnesota, 2013.

24. Leffingwell & Associates, Burnt Sugar, Caramel & Maple Notes, <http://www.leffingwell.com/burnt.htm>, 2013.
25. O. Nishimura and S. Mihara, *Journal of Agricultural and Food Chemistry*, 1990, **38**, 1038-1041.
26. E. M. Suuberg and V. Oja, Federal Energy Technology Center, Morgantown, WV (US); Federal Energy Technology Center, Pittsburgh, PA (US), 1997.
27. P. E. Shaw, J. H. Tatum and R. E. Berry, *Carbohydrate Research*, 1967, **5**, 266-273.
28. K. Niemela, *Carbohydrate Research*, 1988, **184**, 131-137.
29. M. S. Mettler, S. H. Mushrif, A. D. Paulsen, A. D. Javadekar, D. G. Vlachos and P. J. Dauenhauer, *Energy & Environmental Science*, 2012, **5**, 5414-5424.
30. P. R. Patwardhan, D. L. Dalluge, B. H. Shanks and R. C. Brown, *Bioresource Technology*, 2011, **102**, 5265-5269.
31. D. M. Alonso, J. Q. Bond and J. A. Dumesic, *Green Chemistry*, 2010, **12**, 1493-1513.
32. C. Branca, A. Galgano, C. Blasi, M. Esposito and C. Di Blasi, *Energy & Fuels*, 2010, **25**, 359-369.
33. B. R. Simoneit, W. Rogge, M. Mazurek, L. Standley, L. Hildemann and G. Cass, *Environ Sci Technol*, 1993, **27**, 2533-2541.
34. M. Asmadi, H. Kawamoto and S. Saka, *Journal of Analytical and Applied Pyrolysis*, 2011, **92**, 417-425.
35. M. Asmadi, H. Kawamoto and S. Saka, *Journal of Analytical and Applied Pyrolysis*, 2011, **92**, 76-87.
36. C. A. Mullen and A. A. Boateng, *Journal of Analytical and Applied Pyrolysis*, 2011, **90**, 197-203.
37. B. Scholze, C. Hanser and D. Meier, *Journal of Analytical and Applied Pyrolysis*, 2001, **58**, 387-400.
38. T. Hosoya, H. Kawamoto and S. Saka, *Journal of Analytical and Applied Pyrolysis*, 2009, **84**, 79-83.
39. T. Hosoya, H. Kawamoto and S. Saka, *Journal of Analytical and Applied Pyrolysis*, 2009, **85**, 237-246.
40. D. J. Nowakowski, J. M. Jones, R. Brydson and A. B. Ross, *Fuel*, 2007, **86**, 2389-2402.
41. J. P. Diebold, I. Thermalchemie and L. National Renewable Energy, *A review of the chemical and physical mechanisms of the storage stability of fast pyrolysis bio-oils*, National Renewable Energy Laboratory, Golden, CO, 2000.
42. A. Demirbaş, *Energy Conversion and Management*, 2000, **41**, 633-646.
43. D. Mohan, C. U. Pittman and P. H. Steele, *Energy & Fuels*, 2006, **20**, 848-889.
44. M. J. Antal and M. Grønli, *Industrial & Engineering Chemistry Research*, 2003, **42**, 1619-1640.
45. S. Zhou, N. B. Osman, H. Li, A. G. McDonald, D. Mourant, C.-Z. Li and M. Garcia-Perez, *Fuel*, 2013, **103**, 512-523.
46. X. Bai, P. Johnston and R. C. Brown, *Journal of Analytical and Applied Pyrolysis*, 2013, **99**, 130-136.
47. X. Bai, P. Johnston, S. Sadula and R. C. Brown, *Journal of Analytical and Applied Pyrolysis*, 2013, **99**, 58-65.
48. V. Oja and E. Suuberg, *Journal of Chemical & Engineering Data*, 1999, **44**, 26-29.
49. Wageningen University, Caramelization, <http://www.food-info.net/uk/colour/caramel.htm>, Accessed August 2013.
50. M. Villamiel, M. D. del Castillo and N. Corzo, in *Food Biochemistry and Food Processing*, Blackwell Publishing, 2007, pp. 71-100.
51. L. W. Kroh, *Food Chemistry*, 1994, **51**, 373-379.
52. J. E. Hodge, *Journal of Agricultural and Food Chemistry*, 1953, **1**, 928-943.

**Lignocellulosic
Biomass****Pyrolysis
Products****Effect of
Acid Infusion**

Sugars



Agglomerated Char



Pyrolytic Lignin

 CO_2 CO H_2O

Non-condensable Gases

Furans *Carboxylic acids*
Ketones *Aldehydes*

Light Oxygenates

